MAP-BASED AUTOMATIC MODULATION CLASSIFICATION FOR WIRELESS ADAPTIVE OFDM SYSTEMS

L. Häring, C. Kisters

Chair of Communication Systems, University Duisburg-Essen, Duisburg, Germany
{haering,christian.kisters}@nts.uni-due.de

ABSTRACT

This manuscript addresses the maximum-a-posteriori-(MAP)-based automatic modulation classification (AMC) for wireless orthogonal frequency division multiplexing (OFDM) systems with adaptive coding and modulation (ACM). The proposed classifier for quadrature amplitude modulation (QAM) schemes which utilizes the channel reciprocity in time-division duplex (TDD) systems requires the knowledge about the joint probabilities of the subcarrier-wise bit efficiencies at the transmitter and receiver side. In contrast to prior heuristic approaches, these probabilities are calculated analytically (with some approximations) if the transmitter and receiver apply the same bit loading algorithm on their erroneously estimated channel state information. Numerical results reveal that the precise knowledge of the joint probabilities improves the reliability of the automatic modulation classifier significantly, especially for high signal-to-noise power ratios (SNR).

***Index Terms*—** OFDM, automatic modulation classification, adaptive coding and modulation, TDD, maximum-a-posteriori

1. INTRODUCTION

OFDM is one of the most prominent transmission technology in current communication standards due to its advantages to combat frequency-selectivity with low receiver complexity [1]. Furthermore, the multicarrier principle enables the adaptation of the coding and modulation schemes per subcarrier- or subgroup leading to a higher data rate and/or link reliability [2, 3, 4, 5]. Since the coding parameters are typically adapted for a larger span of subcarriers, we focus on the more critical subcarrier-wise bit loading here.

In contrast to wired communication scenarios like digital subscriber line (DSL) in which ACM is already established, the time-variant radio channels necessiates a regular update of the so-called bit allocation table (BAT) in wireless systems. Signalling the BAT to the receiver, however, causes a large amount of overhead [6]. An alternative solution is to automatically classify the modulation schemes on each subcarrier solely based upon the signal form of the received signal and channel reciprocity utilizable in TDD mode.

Relation to prior work. A lot of research on AMC has been carried out during the last decades, mainly for military applications [7, 8]. A comprehensive overview of maximum-likelihood- and feature-based algorithms is given in [9]. Most of the work is not related to the specific characteristics of adaptive wireless OFDM systems. In [10], a similar problem has been investigated where the receiver jointly classifies the BAT and decodes the information in a Trellis-based way. Apart from the high complexity and low flexibility of the decoder, the high error probability is caused by the insufficient utilization of the frame structure, namely the fact that the BAT is constant for the whole frame.

This work was supported by the German Research Foundation under grant HA5655/4-1.

Main contributions. In [11] and [12], the authors of this paper have developed an AMC algorithm which is efficient already for short frames. One open issue was to determine the joint probabilities of the subcarrier bandwidth efficiencies at transmitter and receiver side which is needed to fully exploit the channel reciprocity. In [12], a heuristic approach to approximate these parameters was proposed. In this contribution, we extend the calculations, which was firstly referred to but not finished in [10], adopt them to our scenario and determine the joint probabilities analytically. Using the newly found expressions, we can justify the heuristic low-complexity approach in [12] and, moreover, show that the precise knowledge of the joint probabilities increases the classification reliability even more.

Organization of the paper. The paper is organized as follows: Section 2 introduces the signal model and motivates the idea of this paper. In Section 3, the MAP-based modulation classifier which utilizes channel reciprocity in TDD mode is described. The major contribution of this work is given in Section 4 in which the joint probabilities of transmit and receive bandwidth efficiencies are calculated analytically. Section 5 validates the derivation by numerical investigations of the classification reliability of the proposed algorithm. Finally, conclusions are drawn in Section 6.

Notation. $f_x(\cdot)$ denotes the probability density function (pdf) of x; $\lfloor\cdot\rceil$ is the rounding operation.

2. SIGNAL MODEL AND PROBLEM FORMULATION

In a perfectly synchronized OFDM system, the received symbol $d_{n,k}$ on the n-th subcarrier at the k-th OFDM block can be written as:

$$d_{n,k} = H_{n,k} \cdot s_{n,k} + v_{n,k} \ , \tag{1}$$

where $H_{n,k}$, $s_{n,k}$ and $v_{n,k}$ denote the channel transfer function value, the transmit QAM symbol and additive white Gaussian noise on the n-th subcarrier of the k-th block ($1 \leq n \leq N$, $1 \leq k \leq K$).

The considered signal flow at the initiation of ACM is depicted in Fig. 1. In the uplink, the base station (BS) carries out a channel estimation (CE) based on the preamble sent by the mobile station (MS). By using the estimate $\hat{H}_{\mathrm{Tx},n}$, it applies an ACM algorithm and finds the best coding scheme (common for all subcarriers) and the transmit BAT $\mathbf{b}_{\mathrm{Tx}}$ which includes the bandwidth efficiencies $b_{\mathrm{Tx},1}$ to $b_{\mathrm{Tx},N}$. In the downlink, the BS transmits a frame consisting of a preamble and payload data according to the optimal coding scheme and the BAT $\mathbf{b}_{\mathrm{Tx}}$. Based on the channel estimate $\hat{H}_{\mathrm{Rx},n}$, the MS applies the same ACM algorithm as the BS to find the receive BAT $\mathbf{b}_{\mathrm{Rx}}$ (using the same coding scheme as the BS). In order to be able to decode the payload data, the receiver must be synchronized to the transmit parameters. Whereas the coding scheme and the data rate is signalled conventionally – the overhead caused by these single parameter is negligible – we classify the BAT *automatically* using the following MAP approach.

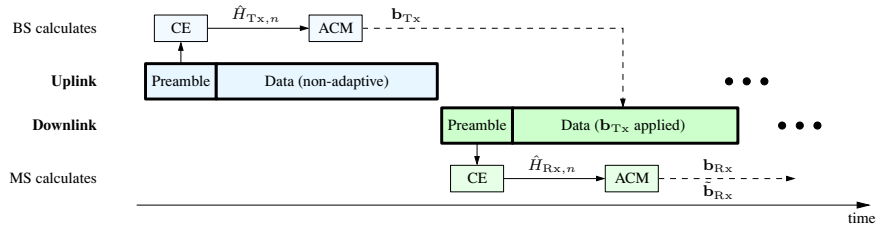

Fig. 1. Considered signal flow in TDD mode at the initiation of adaptive coding and modulation

3. MAP-BASED AUTOMATIC MODULATION CLASSIFICATION

A well-known bit loading algorithm which maximizes the link quality for a given data rate is to adapt the subcarrier bandwidth efficiencies to the channel capacity [2] (here formulated for receiver):

$$b_{\mathrm{Rx},n} = \left\lfloor \tilde{b}_{\mathrm{Rx},n} \right\rceil \quad , \quad \text{s.t.} \quad \frac{1}{N} \cdot \sum_{n=1}^{N} b_{\mathrm{Rx},n} = \bar{b} \tag{2}$$

with

$$\tilde{b}_{\mathrm{Rx},n} = \log_2 \left(1 + k_{\mathrm{Rx}} \cdot |\hat{H}_{\mathrm{Rx},n}|^2\right) , \tag{3}$$

where the factor k_{Rx} is chosen according to the average bandwidth efficiency $\bar{b}$. We assume that the transmitter has applied this loading algorithm analogously for the same data rate.

The proposed AMC algorithm utilizes the symbols $\mathbf{d}_n = [d_{n,1}, \ldots, d_{n,K}]$ and the non-quantized bandwidth efficiencies $\tilde{\mathbf{b}}_{\mathrm{Rx}} = [\tilde{b}_{\mathrm{Rx},1}, \ldots, \tilde{b}_{\mathrm{Rx},N}]$ at the receiver side. The aim of the MAP approach is to search for that hypothesis combination which maximizes the a-posteriori probability $p(\mathbf{b}_{\mathrm{Tx}}|(\mathbf{d}, \tilde{\mathbf{b}}_{\mathrm{Rx}}))$:

$$\hat{\mathbf{b}}_{\mathrm{Tx}} = \underset{\mathbf{b}_{\mathrm{Tx}}}{\operatorname{argmax}}\ p(\mathbf{b}_{\mathrm{Tx}}|(\mathbf{d}, \tilde{\mathbf{b}}_{\mathrm{Rx}})) , \tag{4}$$

where $\mathbf{d} = [\mathbf{d}_1, \ldots, \mathbf{d}_N]$ combines all received symbols. This joint search is not feasible in practical systems. Instead, the subcarrier-independent approach is investigated [12]:

$$\hat{b}_{\mathrm{Tx},n} = \underset{b_{\mathrm{Tx},n}}{\operatorname{argmax}}\ p(b_{\mathrm{Tx},n}|(\mathbf{d}_n, \tilde{b}_{\mathrm{Rx},n})) \tag{5}$$

$$= \underset{b_{\mathrm{Tx},n}}{\operatorname{argmax}}\ \frac{p(b_{\mathrm{Tx},n}, \mathbf{d}_n, \tilde{b}_{\mathrm{Rx},n})}{p(\mathbf{d}_n, \tilde{b}_{\mathrm{Rx},n})} \tag{6}$$

$$= \underset{b_{\mathrm{Tx},n}}{\operatorname{argmax}}\ \underbrace{p(\tilde{b}_{\mathrm{Rx},n}, \mathbf{d}_n, b_{\mathrm{Tx},n})}_{\text{cost function } J} . \tag{7}$$

Thus, the joint probabilitity must be maximized which is:

$$J = p(\tilde{b}_{\mathrm{Rx},n}|(\mathbf{d}_n, b_{\mathrm{Tx},n})) \cdot p(\mathbf{d}_n, b_{\mathrm{Tx},n}) \tag{8}$$

$$= p(\tilde{b}_{\mathrm{Rx},n}|(\mathbf{d}_n, b_{\mathrm{Tx},n})) \cdot p(\mathbf{d}_n|b_{\mathrm{Tx},n}) \cdot p(b_{\mathrm{Tx},n}) . \tag{9}$$

Expanding with $p(\tilde{b}_{\mathrm{Rx},n}, b_{\mathrm{Tx},n})$ and rearranging yields the cost function:

$$J = \frac{p(\tilde{b}_{\mathrm{Rx},n}|(b_{\mathrm{Tx},n}, \mathbf{d}_n))}{p(\tilde{b}_{\mathrm{Rx},n}|b_{\mathrm{Tx},n})} \cdot p(\mathbf{d}_n|b_{\mathrm{Tx},n}) \cdot p(\tilde{b}_{\mathrm{Rx},n}, b_{\mathrm{Tx},n}) . \tag{10}$$

Numerical analysis have shown a good coincidence of the conditional probabilities $p(\tilde{b}_{\mathrm{Rx},n}|(b_{\mathrm{Tx},n}, \mathbf{d}_n))$ and $p(\tilde{b}_{\mathrm{Rx},n}|b_{\mathrm{Tx},n})$. Thus, the considered MAP classifier can be formulated as:

$$\hat{b}_{\mathrm{Tx},n} = \underset{b_{\mathrm{Tx},n}}{\operatorname{argmax}}\ p(\mathbf{d}_n|b_{\mathrm{Tx},n}) \cdot p(\tilde{b}_{\mathrm{Rx},n}, b_{\mathrm{Tx},n}) . \tag{11}$$

The first term in the cost function is the well-known likelihood-function and is derived e. g. in [11]. However, the second term in (11) which describes the amount of reciprocity between transmit and receive BAT could only be heuristically approximated up to now.

4. DERIVATION OF JOINT PROBABILITIES

Problem statement. Suppose that the transmitter and receiver have calculated the subcarrier bandwidth efficiencies according to (3):

$$\tilde{b}_{\mathrm{Tx},n} = \log_2 \left(1 + k_{\mathrm{Tx}} \cdot |\hat{H}_{\mathrm{Tx},n}|^2\right) \tag{12}$$

$$\tilde{b}_{\mathrm{Rx},n} = \log_2 \left(1 + k_{\mathrm{Rx}} \cdot |\hat{H}_{\mathrm{Rx},n}|^2\right) . \tag{13}$$

Now, the joint probabilities $p(\tilde{b}_{\mathrm{Rx},n}, b_{\mathrm{Tx},n})$ are derived under the assumption that the difference between $\tilde{b}_{\mathrm{Tx},n}$ and $\tilde{b}_{\mathrm{Rx},n}$ is only caused by CE errors $\varepsilon_{\mathrm{Tx},n}$ and $\varepsilon_{\mathrm{Rx},n}$ in the time-invariant channel transfer function H_n:

$$\hat{H}_{\mathrm{Tx},n} = H_n + \varepsilon_{\mathrm{Tx},n} \tag{14}$$

$$\hat{H}_{\mathrm{Rx},n} = H_n + \varepsilon_{\mathrm{Rx},n} . \tag{15}$$

Here, we assume channel reciprocity which holds for well-calibrated front-ends in TDD mode. Moreover, we noticed that variations due to the time-variance can be neglected compared to CE errors in typical indoor propagation scenarios with short frames. In case of a zero-forcing (ZF) channel estimator, the error variances $\sigma^2_{\varepsilon_{\mathrm{Tx}}} = \mathrm{E}\{|\varepsilon_{\mathrm{Tx},n}|^2\}$ and $\sigma^2_{\varepsilon_{\mathrm{Rx}}} = \mathrm{E}\{|\varepsilon_{\mathrm{Rx},n}|^2\}$ are inversely proportional to the SNR $\gamma = \mathrm{E}\{|s_{n,k}|^2\}/\mathrm{E}\{|v_{n,k}|^2\}$. For a ZF channel estimator with N_{TS} training blocks and windowing the cyclic prefix with length N_{CP} in the time-domain, it holds [13]:

$$\sigma^2_{\varepsilon_{\mathrm{Tx}}} = \sigma^2_{\varepsilon_{\mathrm{Rx}}} = \frac{1}{N_{\mathrm{TS}} \cdot \frac{N}{N_{\mathrm{CP}}} \cdot \gamma} . \tag{16}$$

4.1. Probability density function $f_{\tilde{b}_{\mathrm{Tx},n}}(\tilde{b}_{\mathrm{Tx},n})$

In the first step, we calculate the probability density function of $\tilde{b}_{\mathrm{Tx},n}$ in terms of the pdf of $|\hat{H}_{\mathrm{Tx},n}|^2$ for a given k_{Tx}:

$$f_{\tilde{b}_{\mathrm{Tx},n}}(\tilde{b}_{\mathrm{Tx},n}) = \frac{f_{|\hat{H}_{\mathrm{Tx},n}|^2}(|\hat{H}_{\mathrm{Tx},n}|^2)}{\left|\frac{\partial \tilde{b}_{\mathrm{Tx},n}}{\partial |\hat{H}_{\mathrm{Tx},n}|^2}\right|} . \tag{17}$$

With the first derivative and the inverse function of (12), respectively,

$$\frac{\partial \tilde{b}_{\mathrm{Tx},n}}{\partial |\hat{H}_{\mathrm{Tx},n}|^2} = \frac{k_{\mathrm{Tx}}}{\ln(2)} \cdot \frac{1}{1 + k_{\mathrm{Tx}} \cdot |\hat{H}_{\mathrm{Tx},n}|^2} \tag{18}$$

$$|\hat{H}_{\mathrm{Tx},n}|^2 = \frac{1}{k_{\mathrm{Tx}}} \cdot \left(2^{\tilde{b}_{\mathrm{Tx},n}} - 1\right) , \tag{19}$$

the pdf of $\tilde{b}_{\mathrm{Tx},n}$ can be written as:

$$f_{\tilde{b}_{\mathrm{Tx},n}}(\tilde{b}_{\mathrm{Tx},n}) = f_{|\hat{H}_{\mathrm{Tx},n}|^2}\left(\frac{2^{\tilde{b}_{\mathrm{Tx},n}}-1}{k_{\mathrm{Tx}}}\right)\cdot\frac{\ln(2)\cdot 2^{\tilde{b}_{\mathrm{Tx},n}}}{k_{\mathrm{Tx}}}\ . \quad (20)$$

For Rayleigh fading, the pdf of $|H_n|^2$ and, due to independent Gaussian estimation error $\varepsilon_{\mathrm{Tx},n}$ also $|\hat{H}_{\mathrm{Tx},n}|^2$, exhibits an exponential function for $h \geq 0$:

$$f_{|\hat{H}_{\mathrm{Tx},n}|^2}(h) = \frac{1}{\sigma^2_{\hat{H}_{\mathrm{Tx}}}}\cdot\exp\left(-\frac{h}{\sigma^2_{\hat{H}_{\mathrm{Tx}}}}\right) \quad (21)$$

with the variance

$$\sigma^2_{\hat{H}_{\mathrm{Tx},n}} = \mathrm{E}\left\{|H_n+\varepsilon_{\mathrm{Tx},n}|^2\right\} = 1+\sigma^2_{\varepsilon_{\mathrm{Tx}}}\ , \quad (22)$$

where $\mathrm{E}\{|H_n|^2\}=1$. Inserting in (20) yields for $\tilde{b}_{\mathrm{Tx},n}\geq 0$:

$$f_{\tilde{b}_{\mathrm{Tx},n}}(\tilde{b}_{\mathrm{Tx},n}) = \frac{\ln(2)\cdot 2^{\tilde{b}_{\mathrm{Tx},n}}}{(1+\sigma^2_{\varepsilon_{\mathrm{Tx}}})\cdot k_{\mathrm{Tx}}}\cdot\exp\left(-\frac{2^{\tilde{b}_{\mathrm{Tx},n}}-1}{(1+\sigma^2_{\varepsilon_{\mathrm{Tx}}})\cdot k_{\mathrm{Tx}}}\right)\ . \quad (23)$$

4.2. Conditional pdf $f_{\tilde{b}_{\mathrm{Rx},n}|\tilde{b}_{\mathrm{Tx},n}}(\tilde{b}_{\mathrm{Rx},n})$

The second step is to calculate the conditional pdf of $\tilde{b}_{\mathrm{Rx},n}$ under the condition $\tilde{b}_{\mathrm{Tx},n}$. The variables $\hat{H}_{\mathrm{Rx},n}$ and $\hat{H}_{\mathrm{Tx},n}$ in (14) and (15) are multivariate Gaussian distributed according to:

$$\begin{pmatrix}\hat{H}_{\mathrm{Rx},n}\\ \hat{H}_{\mathrm{Tx},n}\end{pmatrix} \sim \mathcal{CN}\left(\begin{pmatrix}\mu_1\\ \mu_2\end{pmatrix},\begin{pmatrix}C_{11} & C_{12}\\ C_{21} & C_{22}\end{pmatrix}\right)\ . \quad (24)$$

with $\mu_1=\mu_2=0$, $C_{12}=C_{21}=1$, $C_{11}=1+\sigma^2_{\varepsilon_{\mathrm{Rx}}}$ and $C_{22}=1+\sigma^2_{\varepsilon_{\mathrm{Tx}}}$. Then, the conditional random variable $\hat{H}_{\mathrm{Rx},n}|\hat{H}_{\mathrm{Tx},n}$ is still Gaussian distributed:

$$\begin{aligned}\hat{H}_{\mathrm{Rx},n}|\hat{H}_{\mathrm{Tx},n} &\sim \mathcal{CN}\Big(\mu_1 + C_{12}C_{22}^{-1}(\hat{H}_{\mathrm{Tx},n}-\mu_2),\\ &\qquad C_{11}-C_{12}C_{22}^{-1}C_{21}\Big) \quad (25)\\ &\sim \mathcal{CN}\left(\frac{\hat{H}_{\mathrm{Tx},n}}{1+\sigma^2_{\varepsilon_{\mathrm{Tx}}}},(1+\sigma^2_{\varepsilon_{\mathrm{Rx}}})-\frac{1}{1+\sigma^2_{\varepsilon_{\mathrm{Tx}}}}\right). \quad (26)\end{aligned}$$

Let $A_{\mathrm{Rx},n}=|\hat{H}_{\mathrm{Rx},n}|$ and $\sigma^2_{\varepsilon}=(1+\sigma^2_{\varepsilon_{\mathrm{Rx}}})-1/(1+\sigma^2_{\varepsilon_{\mathrm{Tx}}})$. Then, the conditional pdf of $A_{\mathrm{Rx},n}|\hat{H}_{\mathrm{Tx},n}$ is Rician distributed:

$$\begin{aligned}f_{A_{\mathrm{Rx},n}|\hat{H}_{\mathrm{Tx},n}}(A_{\mathrm{Rx},n}) &= \frac{2A_{\mathrm{Rx},n}}{\sigma^2_{\tilde{\varepsilon}}}\cdot\exp\left(-\frac{A^2_{\mathrm{Rx},n}+\left|\frac{\hat{H}_{\mathrm{Tx},n}}{1+\sigma^2_{\varepsilon_{\mathrm{Tx}}}}\right|^2}{\sigma^2_{\tilde{\varepsilon}}}\right)\\ &\quad\cdot\mathrm{I}_0\left(\frac{2A_{\mathrm{Rx},n}\left|\frac{\hat{H}_{\mathrm{Tx},n}}{1+\sigma^2_{\varepsilon_{\mathrm{Tx}}}}\right|}{\sigma^2_{\tilde{\varepsilon}}}\right), \quad (27)\end{aligned}$$

where $\mathrm{I}_0(\cdot)$ denotes the modified Bessel function of first kind with 0^{th} order: $\mathrm{I}_0(x)=\frac{1}{\pi}\cdot\int_0^{\pi}\mathrm{e}^{x\cdot\cos(t)}\,\mathrm{d}t$. With the inverse function of (13) and the first derivative

$$\begin{aligned}A_{\mathrm{Rx},n} &= \sqrt{\frac{1}{k_{\mathrm{Rx}}}\cdot\left(2^{\tilde{b}_{\mathrm{Rx},n}}-1\right)} \quad (28)\\ \frac{\partial\tilde{b}_{\mathrm{Rx},n}}{A_{\mathrm{Rx},n}} &= \frac{2}{\ln(2)}\cdot\frac{\sqrt{k_{\mathrm{Rx}}\cdot\left(2^{\tilde{b}_{\mathrm{Rx},n}}-1\right)}}{2^{\tilde{b}_{\mathrm{Rx},n}}}\ , \quad (29)\end{aligned}$$

the conditional pdf $f_{\tilde{b}_{\mathrm{Rx},n}|\hat{H}_{\mathrm{Tx},n}}(b)$ is given by:

$$\begin{aligned}f_{\tilde{b}_{\mathrm{Rx},n}|\hat{H}_{\mathrm{Tx},n}}(b) &= \frac{\ln(2)\cdot 2^b}{\sigma^2_{\tilde{\varepsilon}}\cdot k_{\mathrm{Rx}}}\cdot\exp\left(-\frac{\frac{1}{k_{\mathrm{Rx}}}\cdot\left(2^b-1\right)+\left|\frac{\hat{H}_{\mathrm{Tx},n}}{1+\sigma^2_{\varepsilon_{\mathrm{Tx}}}}\right|^2}{\sigma^2_{\tilde{\varepsilon}}}\right)\\ &\quad\cdot\mathrm{I}_0\left(\frac{2\sqrt{\frac{1}{k_{\mathrm{Rx}}}\cdot\left(2^b-1\right)}\left|\frac{\hat{H}_{\mathrm{Tx},n}}{1+\sigma^2_{\varepsilon_{\mathrm{Tx}}}}\right|}{\sigma^2_{\tilde{\varepsilon}}}\right). \quad (30)\end{aligned}$$

By replacing $|\hat{H}_{\mathrm{Tx},n}|$ with $\sqrt{(2^{\tilde{b}_{\mathrm{Tx},n}}-1)/k_{\mathrm{Tx}}}$ according to (12) and setting $A_{\mathrm{Tx},n}=|\hat{H}_{\mathrm{Tx},n}/(1+\sigma^2_{\varepsilon_{\mathrm{Tx}}})|$, the conditional pdf $f_{\tilde{b}_{\mathrm{Rx},n}|\tilde{b}_{\mathrm{Tx},n}}(\tilde{b}_{\mathrm{Rx},n})$ is formulated as:

$$\begin{aligned}f_{\tilde{b}_{\mathrm{Rx},n}|\tilde{b}_{\mathrm{Tx},n}}(\tilde{b}_{\mathrm{Rx},n}) &= \frac{\ln(2)\cdot 2^{\tilde{b}_{\mathrm{Rx},n}}}{\sigma^2_{\tilde{\varepsilon}}\cdot k_{\mathrm{Rx}}}\cdot\exp\left(-\frac{A^2_{\mathrm{Rx},n}+A^2_{\mathrm{Tx},n}}{\sigma^2_{\tilde{\varepsilon}}}\right)\\ &\quad\cdot\mathrm{I}_0\left(\frac{2A_{\mathrm{Rx},n}\cdot A_{\mathrm{Tx},n}}{\sigma^2_{\tilde{\varepsilon}}}\right)\ . \quad (31)\end{aligned}$$

4.3. Joint probabilities $p(\tilde{b}_{\mathrm{Rx},n}, b_{\mathrm{Tx},n})$

The joint pdf of $\tilde{b}_{\mathrm{Tx},n}$ and $\tilde{b}_{\mathrm{Rx},n}$ is then:

$$f_{\tilde{b}_{\mathrm{Rx},n},\tilde{b}_{\mathrm{Tx},n}}(\tilde{b}_{\mathrm{Rx},n},\tilde{b}_{\mathrm{Tx},n}) = f_{\tilde{b}_{\mathrm{Rx},n}|\tilde{b}_{\mathrm{Tx},n}}(\tilde{b}_{\mathrm{Rx},n})\cdot f_{\tilde{b}_{\mathrm{Tx},n}}(\tilde{b}_{\mathrm{Tx},n})\,. \quad (32)$$

In order to take the rounding operation in (2) into account, we finally integrate the joint pdf in the corresponding interval (e. g. $b_{\mathrm{Tx},n}-0.5\leq\tilde{b}_{\mathrm{Tx},n}\leq b_{\mathrm{Tx},n}+0.5$) to determine the joint probabilities:

$$p(\tilde{b}_{\mathrm{Rx},n}, b_{\mathrm{Tx},n}) = \int f_{\tilde{b}_{\mathrm{Rx},n},\tilde{b}_{\mathrm{Tx},n}}(\tilde{b}_{\mathrm{Rx},n},\tilde{b}_{\mathrm{Tx},n})\,\mathrm{d}\tilde{b}_{\mathrm{Tx},n}\ . \quad (33)$$

4.4. Approximation of k_{Tx} and k_{Rx}

Note that the calculated probabilities depend on the factors k_{Tx} and k_{Rx}, respectively. In order to simplify the following calculations, we set $k_{\mathrm{Tx}}=k_{\mathrm{Rx}}=k$. Since it is extremely difficult to find the pdf of k based on the side condition in (2), we restrict ourselves in our analysis to the value of k in the average sense. Despite this simplification, numerical investigations indicate a good agreement of simulation and analytical results. Still, the evaluation of k is difficult in the general case. Therefore, we distinguish different cases:

High capacity approximation. For large bandwidth efficiencies, the approximation $\log_2(1+x)\approx\log_2(x)$ can be used. Then, the expectation of the side condition in (2) w.r.t. different channel realizations and neglecting the rounding operation is:

$$\begin{aligned}\overline{b} &\approx \frac{1}{N}\sum_{n=1}^{N}\mathrm{E}\{\log_2(k\cdot|\hat{H}_{\mathrm{Rx},n}|^2)\} \quad (34)\\ &= \frac{1}{N}\sum_{n=1}^{N}\int_0^{\infty}\log_2(k\cdot h)\cdot\frac{1}{1+\sigma^2_{\varepsilon_{\mathrm{Rx}}}}\mathrm{e}^{-\frac{h}{1+\sigma^2_{\varepsilon_{\mathrm{Rx}}}}}\,\mathrm{d}h\ . \quad (35)\end{aligned}$$

Splitting $\log_2(k\cdot h)=\log_2(k)+\log_2(h)$ and some straightforward calculations, we find

$$\overline{b} \approx \log_2(k)+\log_2(1+\sigma^2_{\varepsilon_{\mathrm{Rx}}})-\frac{1}{\ln(2)}\cdot\mathrm{C}\,, \quad (36)$$

where $\mathrm{C}=-\int_0^{\infty}\ln(x)\exp(-x)\,\mathrm{d}x$ is the Euler constant. Thus, k can be approximated by

$$k\approx 2^{\overline{b}-\log_2(1+\sigma^2_{\varepsilon_{\mathrm{Rx}}})+\frac{1}{\ln(2)}\cdot\mathrm{C}}\ . \quad (37)$$

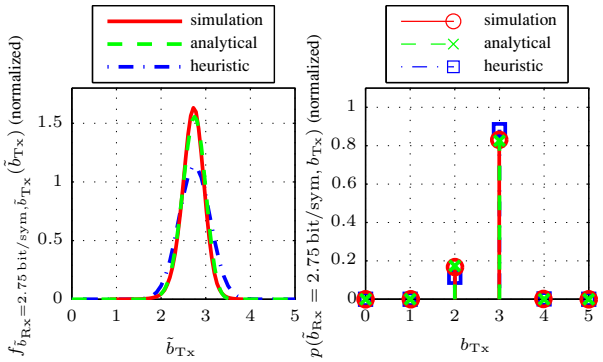

Fig. 2. Example of joint probabilities for small capacity approximation, $\overline{b} = 2\,\mathrm{bit/sym}$ (4-QAM), $\gamma = 10\,\mathrm{dB}$

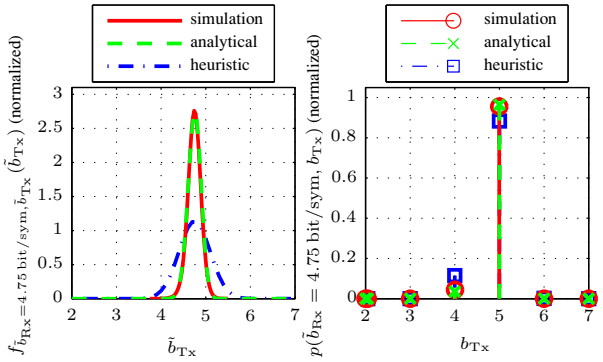

Fig. 3. Example of joint probabilities for high capacity approximation, $\overline{b} = 6\,\mathrm{bit/sym}$ (64-QAM), $\gamma = 20\,\mathrm{dB}$

Small capacity approximation. For small bandwidth efficiencies, $\log_2(1+x) \approx \alpha \cdot x^{\beta}$ with e. g. $\alpha = 1$ and $\beta = 1/2$ is valid [14]. Following the same steps as in the previous paragraph, we have:

$$\overline{b} \approx \frac{1}{N}\sum_{n=1}^{N} \mathrm{E}\left\{\alpha \cdot \left(k \cdot |\hat{H}_{\mathrm{Rx},n}|^2\right)^{\beta}\right\} \tag{38}$$

$$= \frac{1}{N}\sum_{n=1}^{N} \int_0^{\infty} \alpha \cdot (k\cdot h)^{\beta} \cdot \frac{1}{1+\sigma^2_{\tilde{\varepsilon}_{\mathrm{Rx}}}} \cdot \mathrm{e}^{-\frac{h}{1+\sigma^2_{\tilde{\varepsilon}_{\mathrm{Rx}}}}}\,\mathrm{d}h\,. \tag{39}$$

After some manipulations, k can be approximated by:

$$k \approx \frac{1}{1+\sigma^2_{\tilde{\varepsilon}}} \cdot \left(\frac{1}{\alpha \cdot \int_0^{\infty} h^{\beta}\cdot \mathrm{e}^{-h}\,\mathrm{d}h}\right)^{1/\beta} \cdot \overline{b}^{\,1/\beta}\,. \tag{40}$$

Based on the chosen α and β, the integral can be calculated offline. E.g., for $\alpha = 1$ and $\beta = 1/2$, it holds:

$$k \overset{\alpha=1,\beta=1/2}{\approx} \frac{1.27}{1+\sigma^2_{\tilde{\varepsilon}}} \cdot \overline{b}^{\,2}\,. \tag{41}$$

5. NUMERICAL RESULTS

The OFDM relevant simulation parameters are concordant to the IEEE 802.11a/n standard: sampling period of $T = 50\,\mathrm{ns}$, $N = 64$ and a cyclic prefix length of $N_{\mathrm{CP}} = 16$. The multipath channel is based on indoor propagation model B in [15] with a Doppler frequency of $f_{\mathrm{dop}} = 20\,\mathrm{Hz}$. It is estimated using a ZF algorithm and uses two preamble OFDM blocks: $N_{\mathrm{TS}} = 2$. The number of payload OFDM blocks is $K = 20$. The code rate is chosen according to the principle in [5]; bit loading like in [2] with bandwidth efficiencies between 0 and 10 bit/sym follows in a second step.

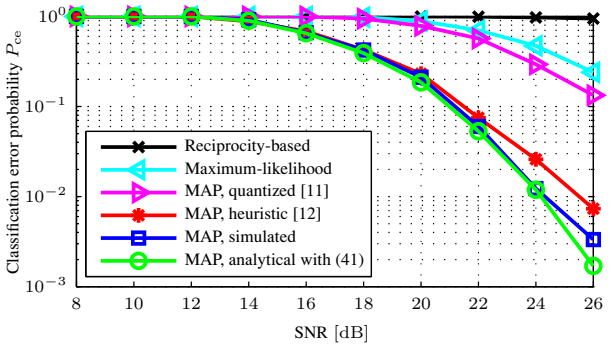

Fig. 4. Classification error probability $P_{\mathrm{ce}} = P(\hat{\mathbf{b}}_{\mathrm{Tx}} \neq \mathbf{b}_{\mathrm{Tx}})$ versus transmit SNR for different AMC algorithms

In order to show the validity of the analytical results, Fig. 2 and Fig. 3 depict two examples of the joint pdf of $\tilde{b}_{\mathrm{Rx},n}$ and $\tilde{b}_{\mathrm{Tx},n}$ and the probabilities $p(\tilde{b}_{\mathrm{Rx},n}, b_{\mathrm{Tx},n})$ for different fixed receive bandwidth efficiencies $\tilde{b}_{\mathrm{Rx},n}$, average bandwidth efficiencies $\overline{b}$ and SNR values. It can be seen that the analytical and simulation results agree very well. The heuristic approach in [12] which assumes a Gaussian error distribution with fixed variance is reasonable but clearly suboptimal. Note that for smaller SNR, the shape of the joint pdf deviates significantly from a Gaussian characteristic (not shown here). Fig. 4 depicts the classification error probability $P_{\mathrm{ce}} = P(\hat{\mathbf{b}}_{\mathrm{Tx}} \neq \mathbf{b}_{\mathrm{Tx}})$ versus the transmit SNR for different AMC algorithms and an average bandwidth efficiency of $\overline{b} = 4\,\mathrm{bit/sym}$. Clearly, if either only the received symbols $\mathbf{d}_n$ (*Maximum-likelihood*) or $\mathbf{b}_{\mathrm{Rx}}$ (*Reciprocity-based*) is exploited in the classification, the classification reliability is poor. Using the quantized bit efficiencies $\mathbf{b}_{\mathrm{Rx}}$ instead of $\tilde{\mathbf{b}}_{\mathrm{Rx}}$ (*MAP, quantized*) [11] also leads to a large performance degradation. Moreover, it can be seen that the performance of the novel AMC algorithm using the analytical results of $p(\tilde{b}_{\mathrm{Rx},n}, b_{\mathrm{Tx},n})$ (*MAP, analytical*) is similar to using the simulated joint probabilities (*MAP, simulated*). Coincidentally, it performes even slightly better which comes from the suboptimality of subcarrier-independent approach and the simplification in (11). Both algorithms outperform the heuristic approach (*MAP, heuristic*), especially at higher SNRs.

6. CONCLUSIONS

This paper focuses on the MAP-based automatic modulation classification for adaptive OFDM systems. In order to fully exploit channel reciprocity in the considered TDD system, the joint probabilities of the transmit and receive subcarrier bandwidth efficiencies must be precisely known. The analytical calculation in this contribution gives more insight in the amount of reciprocity and is a substantial enhancement compared to a prior heuristic approximation. Numerical results in terms of the classification reliability show a significant improvement when using the analytical expressions, at cost of a higher complexity. In view of its low complexity and high classification reliability, the heuristic approach appears to be a good trade-off for practical applications.

7. REFERENCES

[1] John A. C. Bingham, "Multicarrier modulation for data transmission: An idea whose time has come," *IEEE Communications Magazine*, vol. 28, no. 5, pp. 5–14, May 1990.

[2] P. Chow, J. Cioffi, and J. Bingham, "A practical discrete multitone transceiver loading algorithm for data transmission over spectrally shaped channels," *IEEE Transactions on Communications*, vol. 43, no. 2/3/4, pp. 773–775, Feb./Mar./Apr. 1995.

[3] A. Czylwik, "Adaptive OFDM for wideband radio channels," in *Proc. of Global Telecommunications Conference GLOBECOM '96*, 18–22 Nov. 1996, pp. 713–718.

[4] S. Stiglmayr, M. Bossert, and E. Costa, "Adaptive coding and modulation in OFDM systems using BICM and rate-compatible punctured codes," in *Proc. of European Wireless*, April 2007.

[5] C. Bockelmann, D. Wübben, and K.-D. Kammeyer, "Efficient coded bit and power loading for BICM-OFDM," in *Proc. of Vehicular Technology Conference 2009 Spring*, Barcelona, Spain, April 2009, pp. 1 –5.

[6] Y. Chen, L. Häring, and A. Czylwik, "Reduction of AM-induced signaling overhead in WLAN-based OFDM systems," in *Proceedings of the 14th International OFDM-Workshop (InOWo)*, Hamburg, Germany, Sept. 2009, pp. 30–34.

[7] A.K. Nandi and E.E. Azzouz, "Algorithms for automatic modulation recognition of communication signals," *IEEE Transactions on Communications*, vol. 46, no. 4, pp. 431–436, April 1998.

[8] W. Wei and J.M. Mendel, "Maximum-likelihood classification for digital amplitude-phase modulations," *IEEE Transactions on Communications*, vol. 48, no. 2, pp. 189–193, Feb. 2000.

[9] O. A. Dobre, A. Abdi, Y. Bar-Ness, and W. Su, "Survey of automatic modulation classification techniques: classical approaches and new trends," *IET Communications*, vol. 1, no. 2, pp. 137–156, Apr. 2007.

[10] M. Lampe, *Adaptive Techniques for Modulation and Channel Coding in OFDM Communication Systems*, Ph.D. thesis, Apr. 2004.

[11] L. Häring, Y. Chen, and A. Czylwik, "Automatic modulation classification methods for wireless OFDM systems in TDD mode," *IEEE Trans. on Communications*, vol. 58, no. 9, pp. 2480 – 2485, Sept. 2010.

[12] L. Häring, Y. Chen, and A. Czylwik, "Utilizing side information in modulation classification for wireless OFDM systems with adaptive modulation," in *Proceedings of the IEEE Vehicular Technology Conference 2011 Fall*, San Francisco, USA, Sept. 2011.

[13] K. D. Kammeyer, *Nachrichtenübertragung*, Teubner Verlag, ISBN: 978-3-8351-0179-1, 2008.

[14] M. Dohler and H. Aghvami, "On the approximation of MIMO capacity," *IEEE Transactions on Wireless Communications*, vol. 4, no. 1, pp. 30 – 34, Jan. 2005.

[15] J. Medbo and P. Schramm, "Channel models for HiperLAN/2 in different indoor scenarios," ETSI/BRAN document no. 3ERI085B, Mar. 1998.